Research Article / Mechanical Engineering, Mechatronics, and Materials Science https://doi.org/10.15446/ing.investig.93876

Development of a New Method for Synthesizing HITEC Salt-Based Alumina Nanofluids

Desarrollo de un nuevo método de síntesis de nanofluidos de alúmina a base de sal HITEC

Marllory Isaza-Ruiz[1], and Francisco Bolívar-Osorio[2]

ABSTRACT

This study presents a new two-step method to synthesize molten salt-based nanofluids by replacing water with butanol and using an Emax high-energy mill to ensure good stability and homogeneity. Commercial HITEC molten salt was selected as the base fluid, and alumina nanoparticles (nominal size of 5,1 nm) were used as an additive in three different proportions: 0,5, 1,0, and 1,5 wt.%. The specific heat capacity was evaluated through two different methods: differential scanning calorimetry (DSC) and modulated differential scanning calorimetry (MDSC). According to the evaluation by MDSC, an increment of up to 4,27% in the specific heat capacity was achieved with 1,0 wt.% of alumina nanoparticles in comparison with the raw salt, without affecting the melting point and thermal stability of the salt. This behavior may be related to the good distribution of the nanoparticles in the salt. However, no significant improvement in the specific heat capacity of the nanofluid was observed when the standard DSC method was applied. This behavior may be due to the different sensitivities of the two methods to small changes in the sample, with MDSC being the more sensitive technique, as it establishes the contribution of the two phases that make up the nanofluid: the molten salt as the base fluid and the solid nanoparticles. Similarly, the heating rate used in each of the techniques can influence the sensitivity with regard to determining changes in nanofluids.

Keywords: DSC, MDSC, molten salt-based nanofluids, specific heat capacity

RESUMEN

Este estudio presenta un nuevo método de dos pasos para sintetizar nanofluidos a base de sales fundidas reemplazando el agua por butanol y utilizando un molino de alta energía Emax para garantizar una buena estabilidad y homogeneidad. Se seleccionó la sal fundida comercial HITEC como fluido base y se utilizaron nanopartículas de alúmina (tamaño nominal de 5,1 nm) como aditivo en tres proporciones diferentes: 0,5, 1,0 y 1,5 % en peso. La capacidad calorífica específica se evaluó mediante dos métodos diferentes: calorimetría diferencial de barrido (DSC) y calorimetría diferencial de barrido modulada (MDSC). Según la evaluación por MDSC, se logró un incremento de hasta 4,27 % en la capacidad calorífica específica con 1,0 % en peso de nanopartículas de alúmina en comparación con la sal pura, sin afectar el punto de fusión y estabilidad térmica de la sal. Este comportamiento puede estar relacionado con la buena distribución de las nanopartículas en la sal. Sin embargo, no se observó una mejora significativa en la capacidad calorífica específica del nanofluido cuando se aplicó el método estándar de DSC. Este comportamiento puede deberse a las diferentes sensibilidades de los dos métodos a pequeños cambios en la muestra, siendo MDSC la técnica más sensible, ya que establece el aporte de las dos fases que componen el nanofluido: la sal fundida como fluido base y las nanopartículas sólidas. Del mismo modo, la velocidad de calentamiento utilizada en cada una de las técnicas puede influir en la sensibilidad para determinar cambios en los nanofluidos.

Palabras clave: DSC, MDSC, nanofluidos a base de sales fundidas, capacidad calorífica específica

Received: February 2nd, 2021
Accepted: March 4th, 2022

Introduction

Due to global energy shortages and the unstable energy supply, as well as to concerns over environmental pollution, renewable energies have drawn the attention of researchers as a way to obtain sustainable energy sources. Concentrated solar power energy (CSP) stands out among the renewable energies that have been studied thanks to its advancing development and annual production, reaching 6,2 GW in 2020 (REN21, 2021). Nevertheless, as a result of the sun's intermittency, it is necessary to use a profitable storage system with which is possible to increase the efficiency and conservation of energy as well as the competitiveness

[1] Materials engineer, Universidad de Antioquia, Medellín, Colombia. PhD in Materials Engineering, Universidad de Antioquia, Medellín, Colombia. Affiliation: Microscopist, Centro de Microscopia Avanzada, CAM, Universidad de Antioquia, Medellín, Colombia. Email: marllory.isazar@udea.edu.co

[2] Metallurgical engineer, Universidad de Antioquia, Medellín, Colombia. PhD in Materials Physics, Universidad Complutense de Madrid, Madrid, España. Affiliation: Associate professor, Universidad de Antioquia, Medellín, Colombia. Email: francisco.bolivar@udea.edu.co

How to cite: Isaza-Ruiz, M., and Bolívar-Osorio, F. (2023). Development of a new method for synthesizing HITEC salt-based alumina nanofluids. *Ingeniería e Investigación, 43*(1), e93876. https://doi.org/10.15446/ing.investig.93876

of CSP compared to traditional sources. To improve the thermodynamic cycles of solar thermal energy, the use of heat transfer fluids (HTF) based on organic substances such as oils has been replaced with the use of molten salts such as nitrates and nitrites, given their high thermal stability, low vapor pressure, chemical inertness, availability, and profitability. However, these salts have low specific heat capacity and low thermal conductivity, so they are still under study (Serrano-López *et al*., 2013).

The use of solid nanoparticles (less than 100 nm in size) to obtain nanofluids with molten salt as base fluid –thereby improving the thermal properties of the molten salt– has been studied by several authors (Chieruzzi *et al*., 2017a; Hu *et al*., 2017; Zhang *et al*., 2017). Ho and Pan (2017) showed that the optimum amount to be added to commercial HITEC salt in order to obtain the best properties was 0,063 wt.% of alumina nanoparticles, through which an increase in the specific heat capacity of 19,9% is obtained. In this study, it was shown that, at higher concentrations of alumina, there is a decrease in the specific heat capacity of the salt. Schuller *et al*. (2015), on the other hand, proved that there is a parabolic relation between the specific heat and the mass fraction of alumina nanoparticles added to nitrate salts, obtaining a maximum specific heat increase of 30,6% with a 0,78 wt.% of alumina.

Although there are several reports on the use of solid additives to improve the properties of the salts used in CSP (Muñoz-Sánchez, Nieto-Maestre, Imbuluzqueta, *et al*., 2017; Schuller *et al*., 2015), only some reports (Betts, 2011; Muñoz-Sánchez *et al*., 2017) show the influence of the method on measuring thermal properties, specifically heat capacity. Regarding the synthesis method typically used for the preparation of nanofluids based on molten salts, the most common is the two-step method, the well-known *dissolution method*, which includes water as a dispersion medium in the process. For this reason, recent research has focused on improving the method by making some modifications without affecting the thermal properties of the nanofluid (Chen *et al*., 2019; Chieruzzi *et al*., 2017b; Navarrete *et al*., 2020). In this vein, different proposed methods including the ball mill dry method and a spray drying method were evaluated by Navarrete *et al*. (2020). Similarly, Chieruzzi *et al*. (2017b) determined an increase in the specific heat capacity of up to 18,6% with 1 wt.% of SiO_2-Al_2O_3 in Solar Salt at high temperatures using a twin-screw micro-compounder. None of these reports used commercial HITEC salt as base salt, and they do not propose an entirely new synthesis method.

Therefore, considering the importance of developing new synthesis methods as well as the current controversy regarding the most suitable method to measure the specific heat capacity (Cp) of molten salt, especially with nanoparticles that are molten salt-based nanofluids (MSBNFs), this work focuses on contributing to the understanding of this property, mainly concerning the commercial molten HITEC salt in comparison with MSBNFs with 0,5, 1,0, and 1,5 wt.%. Alumina nanoparticles were synthesized by means of a new two-step method. The specific heat capacity was evaluated with both scanning differential calorimetry (DSC) according to the ASTM E1269 (ASTM International, 2011) and modulated scanning differential calorimetry (MDSC) according to the ASTM E2716 (ASTM International, 2015). On the other hand, the melting temperature was measured via DSC, and the thermal stability with and without nanoparticles was evaluated through thermogravimetric analysis (TGA).

Materials and methods

Synthesis

Synthesis of ternary nitrate salt (*HITEC*)

Sodium nitrate (AR ≥ 99,5% purity, Millipore Corporation), sodium nitrite, and potassium nitrate (AR ≥ 99,0% purity, Millipore Corporation) were selected to prepare the eutectic ternary nitrate salt known as HITEC. The eutectic composition in the $NaNO_3$-$NaNO_2$-KNO_3 ternary salt system was synthesized by means of weighted amounts of 7, 40, and 53 mol.%, respectively, and mixing them uniformly in a mortar. The mixtures were then heated in a furnace at a constant heating rate of 5 °C/min from room temperature to 150 °C and held for 1 h until complete fusion was achieved to form the eutectic salts. After that, a heating rate of 3 °C/min to 270 °C and holding for 48 h were used to eliminate the water in the mixture. Finally, two heating and cooling cycles were carried out in a furnace in order to ensure homogeneity in the mixture. Finally, the molten salts were cooled rapidly and pulverized for future experiments.

Synthesis of molten salt-based nanofluids (*MSBNFs*)

To obtain a homogenous mixture between the molten salt and the alumina nanoparticles, a new synthesis method of the nitrate-nitrites molten salt-based nanofluids was developed. Hence, after moisture elimination over 48 h at 270 °C in a furnace, the HITEC molten salt was homogenized and pulverized using a mortar for 20 min and an Emax high-energy mill for 15 min at 300 rpm. Next, the pulverized molten salt was mixed with the alumina nanoparticles (0,5, 1,0, and 1,5 wt.%), which had been previously suspended in butanol and sonicated for at least one hour, using magnetic agitation for 15 min. Finally, the mixture was subjected to two heating and cooling cycles in order to ensure the homogeneity of the MSBNFs and the complete elimination of butanol, using cycles between 160 and 270 °C with 1 h holds. Figure 1 presents the new synthesis method, and Table 1 shows some thermal properties of HITEC and alumina.

Characterization

Transmission electron microscopy (*TEM*)

The size and shape of alumina nanoparticles were observed with an electron transmission microscope (Tecnai F20 Super

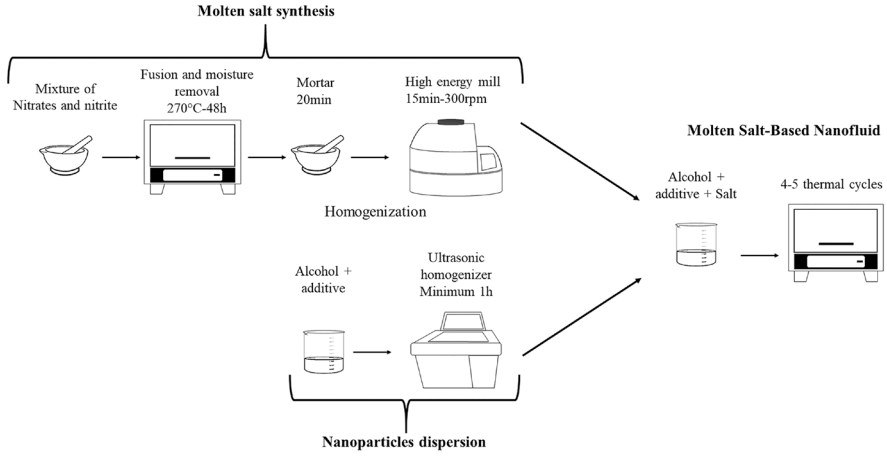

Figure 1. Synthesis method
Source: Authors

Twin, with a field emission source and a resolution of 0,1 nm in 200 Kv TMP). Considering the low solubility of alumina in butanol, the particles were dispersed in it. Then, an aliquot was placed on a copper grid (Lacey carbon mesh 200) and heated long enough to ensure solvent elimination.

Table 1. Thermal properties of HITEC and alumina

Property	HITEC	Alumina
Melting point (˚C)	145,75	2 050 2 072**
Heat capacity (J / g.℃) at 300 ˚C	1,51	0,79
Thermal conductivity (W/m K)	0,2* (at 300˚C)	16,7 (at 306,5˚C)***

* (Vignarooban *et al*., 2015)
** (Larche, 1945)
*** (Myers *et al*., 2016)
Source: Authors

Structural analysis by scanning electron microscopy (SEM)

The samples were fixed on graphite tape, and a thin gold coating (Au) was made using DENTON VACUUM Desk IV equipment. The analysis was performed in a high-vacuum scanning electron microscope (JEOL JSM 6490 LV) to obtain high-resolution images. A secondary electron detector was used to evaluate the morphology and topography of the samples. The elemental analysis was carried out by energy-dispersive X-ray spectroscopy (EDS; INCA PentaFETx3, Oxford Instruments). SEM images were taken from the pristine alumina and the MSBNFs after the DSC and MDSC measurements in order to verify the presence of the nanoparticles inside the molten salt, as well as to evaluate the agglomeration.

Differential scanning calorimetric (DSC) analysis

The melting point of the base fluid and the MSBNFs was measured using a differential scanning calorimeter (Q200, TA Instruments, Inc.). An aluminum Tzero hermetic pan/lid (TA instruments) was used to place the samples in the DSC under a nitrogen atmosphere, and these were analyzed using TA Universal Analyzer 2000, version 4,5 A. The weighting amount for each mixture was around 20 mg for both the base fluid and the MSBNFs. The measurement started at room temperature and increased linearly by 10 ˚C/min up to 400 ˚C, reaching equilibrium at 40 ˚C. The test had a sampling interval every 0,10 s/pt, and two heating and cooling runs were performed to obtain a homogeneous result.

The specific heat capacity of HITEC molten salt and the MSBNFs was measured using two different methods. The first method involved using the traditional differential scanning calorimeter (DSC; Q200, TA Instrument, Inc.) according to the ASTM E1269 standard (ASTM International, 2011). The samples were heated to 250 ˚C and held at this temperature for 5 min in order to obtain a stable heat flux signal, after which they were again heated to 350 ˚C at a rate of 20 ˚C/min. The specific heat of the sample was obtained according to (1), where m_{ref} and m_{Sample} are the standard reference and sample masses, respectively:

$$C_{p,\,sample} = \frac{Q_{sample} - Q_0}{Q_{ref} - Q_0} \cdot \frac{m_{ref}}{m_{sample}} \cdot C_{p,ref} \quad (1)$$

As a second method to measure the Cp of all samples, which involved the modulated differential scanning calorimeter (MDSC), was used according to the ASTM E2716 standard (ASTM International, 2015), with the same equipment used for the DSC analysis. This kind of method uses a sinusoidal temperature oscillation instead of the traditional linear ramp, which simultaneously provides the heat capacity of the sample and the heat flow. The sample was heated to 250 ˚C and held at this temperature for 5 min in order to obtain a stable heat flux signal. After that, the amplitude was ± 0,50 ˚C every 130 s. Finally, the sample was heated again

to 350 ˚C at 2 ˚C/min. The temperature evaluated regarding the specific heat capacity for both methods was 300 ˚C, as it is the temperature at which the salt is commonly maintained in parabolic trough plants.

Thermogravimetric analysis

The thermal stability of pure eutectic salt and the MSBNFs was determined by thermogravimetric analysis (TGA; Q500, TA Instruments, Inc.) under a constant stream of nitrogen at a flow rate of 50 ml/min, a temperature ramp of 15˚C/min in the range 25-800 ˚C, and an isotherm for 5 min. A platinum crucible was used, with weights between 7 and 10 mg for both the HITEC salt and the nanofluid.

Results

Morphology of alumina

The alumina used to synthesize the MSBNFs was obtained from clay minerals by means of an acid leaching process, followed by alkaline precipitation and an acidification process, to finally calcine and obtain mainly delta-gamma alumina with 98,5% purity. The complete procedure was reported by Botero *et al*. (2020). Figure 2a and 2b show the SEM and TEM images of the pristine alumina nanoparticles used to elaborate the MSBNFs, respectively, and Figure 2c shows the size distribution (average size of 5,1 nm). The regular shape can be observed in the SEM and TEM images.

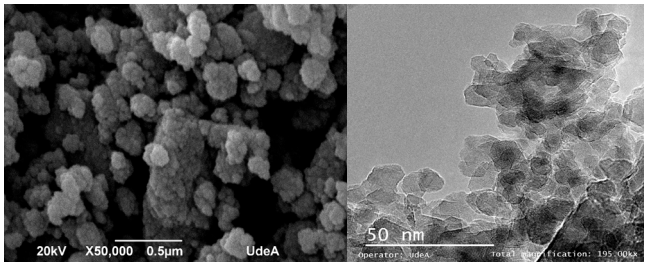

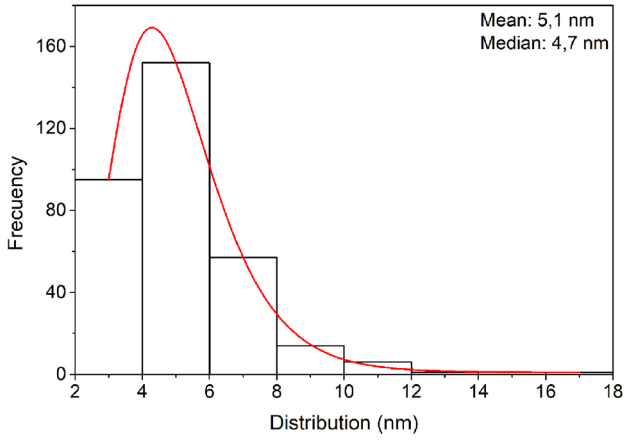

Figure 2. Pristine alumina nanoparticles are used to elaborate the MSBNFs: a) SEM image, b) TEM image, and c) the size distribution
Source: Authors

Thermal stability

The results of the TGA experiments are summarized in Table 2 and Figure 3. In order to evaluate the thermal stability of both the molten salt HITEC and the MSBNFs with 0,5, 1,0, and 1,5 wt.% of alumina nanoparticles, the maximum stability temperature criterion was used when 3% of the overall weight had been lost (Villada *et al*., 2019), whereby a temperature of 300 ˚C was chosen as the initial temperature at which the mass loss started. Based on this criterion, the thermal stability of HITEC salt under the N_2 atmosphere was 626,48 ˚C, which is higher than the results reported in the literature (about 454 ˚C, with a maximum of 535-538 ˚C) (Chen *et al*., 2018), whereas the thermal stability for the MSBNFs was higher than 636 ˚C. The discrepancies in the thermal stability of pure HITEC salt have been explained by Villada *et al*. (2018), and, in order to prevent the conversion of nitrite ions into nitrate ones, HITEC salt should be in an oxygen-free atmosphere. As it can be observed, pure HITEC salt and MSBNFs exhibit a similar decomposition behavior, with a slight increase in the maximum temperature of up to 2% with 1,5 wt.% of alumina nanoparticles. This behavior, together with the reduced melting point, extends the working temperature range of the material, which makes the resulting mixture of potential interest for CSP applications.

Table 2. TGA results for HITEC and MSBNFs with 0,5, 1,0, and 1,5 wt.% of alumina nanoparticles under a nitrogen atmosphere

Sample	Thermal decomposition (˚C)	Change percentage (%)
HITEC (H)	626,48	-
H+0,5% Al_2O_3	636,12	1,54
H+1,0% Al_2O_3	636,93	1,67
H+1,5% Al_2O_3	639,02	2,00

Source: Authors

Melting temperature

The melting temperature values of the HITEC molten salt and the MSBNFs were obtained via DSC. Two heating and cooling runs were carried out to avoid discrepancies in the melting temperature produced by the hygroscopic property of some nitrates. The first cycle was performed to achieve the perfect incorporation of the mixture, and the results from this sequence were not considered. The other cycle was analyzed, and the data from these runs are reported in Table 3.

onsidering previous reports made by Gimenez and Fereres (2015) and Mohammad *et al*. (2017), the heating rate affects the onset of melting, as well as the height and width of the peaks and transition enthalpies. As both the base molten salt (HITEC) and the nanofluids with the different alumina nanoparticle concentrations are not pure materials, the melting temperature of the sample is taken as the endset temperature of the main endothermic peak at the DSC curve

(Bonk *et al.*, 2018). Therefore, according to the literature, the melting point corresponding to the HITEC salt was 145,75 ˚C (Coastal Chemical Co. LLC, 2009; Fernández *et al.*, 2015), and the endset point was 149,82 ˚C.

Table 3. Melting point of HITEC and MSBNFs with 0,5, 1,0, and 1,5 wt.% alumina nanoparticles

Sample	Melting point (˚C)	Onset (˚C)	Endset (˚C)
HITEC (H)	145,75	139,37	149,82
H+0,5% Al_2O_3	145,42	137,13	148,88
H+1,0% Al_2O_3	140,90	133,61	147,83
H+1,5% Al_2O_3	140,52	133,31	147,41

Source: Authors

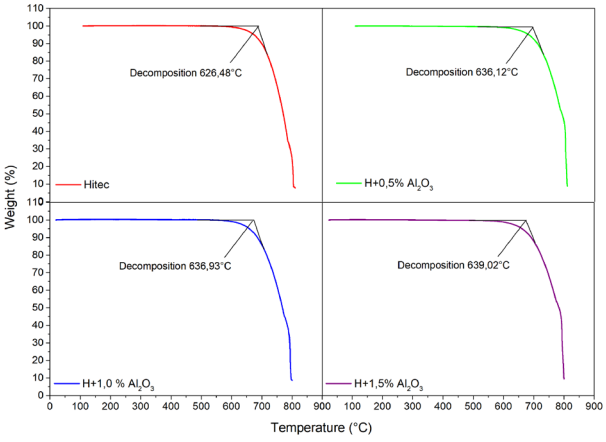

Figure 3. Decomposition temperature under N_2 atmosphere of the pure HITEC salt and the MSBNFs with 0,5, 1,0 and 1,5 wt.% of alumina nanoparticles
Source: Authors

The increase from 0,5 to 1,5 wt.% of alumina leads to a reduction of the onset, endset, and melting point temperatures. This effect was observed in all three concentrations under study, but it was more evident for 1,5 wt.% of nanoparticles (up to 3,6% compared to the base salt mixture). However, this behavior does not correspond to the reports of some authors (Chieruzzi *et al.*, 2013), in which there is a higher enhancement of the thermal properties of the molten salt with 1,0 wt.% and thermal properties start to be negatively affected with a greater amount of nanoparticles. In particular, the onset temperature decreased when Al_2O_3 was added. This means that the phase change occurs at a lower temperature in comparison with the base salt, which is a clear advantage for applications in CSP plants.

Specific heat capacity

The specific heat capacity of the MSBNFs synthesized with HITEC as a base fluid and alumina nanoparticles with a nominal size of 5,1 nm in three different proportions (0,5, 1,0, and 1,5 wt.%) was determined by two different methods: traditional differential scanning calorimetry (DSC) according to the ASTM E1269 standard (ASTM International, 2011) and modulated differential scanning calorimetry (MDSC) according to ASTM E2716 (ASTM International, 2015). The results shown in Table 4 correspond to the Cp values at 300 ˚C, a temperature chosen since it is a normal operating temperature in parabolic trough collectors at the point where the salt is completely melted and without any water content.

Table 4. Heat capacity results in DSC and MDSC

Sample	Heat Capacity (J/g ˚C)			
	DSC	Relative error	MDSC	Relative error
HITEC (H)	1,510	0,0871	1,510	0,0164
H+0,5% Al_2O_3	1,506	0,1817	1,549	0,0563
H+1,0% Al_2O_3	1,508	0,1097	1,577	0,1192
H+1,5% Al_2O_3	1,499	0,0670	1,565	0,0924

Source: Authors

To compare both methods and consider the ASTM E1269 and ASTM E2716 standards, Table 4 reports the average of three different measurements of the same sample, ensuring that the mass loss in every measure does not exceed 0,3% of the initial mass. Therefore, the average deviation is small compared to what is normally reported in the literature. In this way, the result obtained by HITEC commercial salt (1,51 J/g˚C at 300 ˚C) was consistent with the value reported by Kearney *et al.* (2002). On the other hand, the good sensitivity and low uncertainty of the MDSC method reported by Muñoz-Sánchez *et al.* (2017) are also demonstrated in this research.

It should be noted that the weighted amount for each measurement performed was 20 mg in order to ensure that, once melted, the sample remained at the center of the crucible, thus establishing good contact between the sample and the sensor throughout the test (Muñoz-Sánchez *et al.*, 2017). As shown in Table 4, the specific heat capacity of the MSBNFs evaluated through the MDSC method increased along with the proportion of nanoparticles: up to 4,56% with 1 wt.% of Al_2O_3, showing a limit close to 1 wt.% of nanoparticles, with a slight reduction of Cp with 1,5 wt.% of alumina. This behavior has been demonstrated with other kinds of nanofluids, particularly with commercial Solar Salt as base fluid (Awad *et al.*, 2018; Hu *et al.*, 2019). On the other hand, this effect is not so obvious when using standard DSC, where a similar increase in Cp was obtained for all the percentages of nanoparticles evaluated, with a maximum increase up to 0,53% with 1,0 wt.%. Furthermore, it is important to highlight that both methods were not applied

at the same heating rate because the norm for the traditional method was followed. However, this difference in speed can lead to the MDSC method being more sensitive than the traditional DSC.

The low increases in Cp obtained in this study compared to those reported by other authors may be due to several reasons. Firstly, the employed alumina was not 100% pure, and some studies have reported that impurities in the base salts can affect the thermophysical properties of the MSBNFs (Muñoz-Sánchez *et al.*, 2017; Muñoz-Sánchez *et al.*, 2018). The impurities within the alumina can also have a negative effect on the Cp of the MSBNFs, which is why this method must be verified with 100% pure alumina. Secondly, the size of the alumina was less than what is commonly used, although some authors have indicated that nanoparticle size is not a determining factor for the Cp value (Seo and Shin, 2016; Tiznobaik and Shin, 2013), while others indicate that the Cp is higher with larger nanoparticles (Dudda and Shin, 2013; Lu and Huang, 2013). However, the specific heat has been demonstrated to depend on the specific surface available, and thus on the size of the agglomerates formed during the production of the MSBNFs, as indicated by Andreu-Cabedo *et al.* (2014). It should be noted that the size of the agglomerates depends on the synthesis method, which may imply that the improvement in the specific heat may be due to the formation of agglomerates attributed to the use of butanol, which, together with the high heating rate of the DSC method, does not lead to an apparent improvement, although it is possible to observe using the MDSC method at a lower heating rate.

Finally, the new method is presented –which is used for the first time– in which the nanoparticles are dispersed by butanol. This process must be optimized and thoroughly evaluated in order to understand its repercussions. However, the increase of up to 4,56% in Cp shows that the method is suitable for use in the synthesis of MSBNFS for thermal storage, with the purpose of improving the efficiency of TES systems.

Considering the direct relationship between the behavior of the specific heat capacity with the phase and structure of the material, SEM was used to perform the microstructural analysis of both the HITEC pure molten salt and the MSBNFs. In the same way, the analysis of the degree of dispersion of nanoparticles in the molten salt after the Cp evaluation using both the DSC and MDSC methods was carried out using SEM. Figure 4 shows the SEM images of the commercial HITEC molten salt, and Figure 5 shows the SEM images of the MSBNFs, with 5a, 5b, and 5c being the samples evaluated by DSC, and 5d, 5e, and 5f corresponding to the samples evaluated by MDSC.

However, neither the interconnecting network of nanoparticles nor the needle-like structure were observed in the nanofluids, factors reported by other authors as the possible cause of Cp enhancement with nanoparticles (Shin and Banerjee, 2014; Song *et al.*, 2018). At the same time,

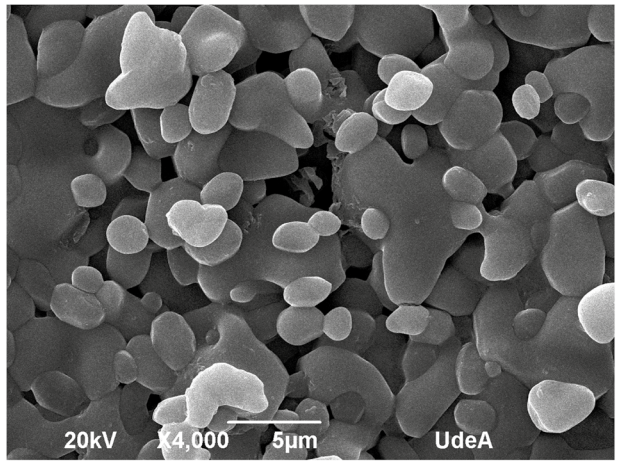

Figure 4. SEM Images of pure commercial HITEC salt
Source: Authors

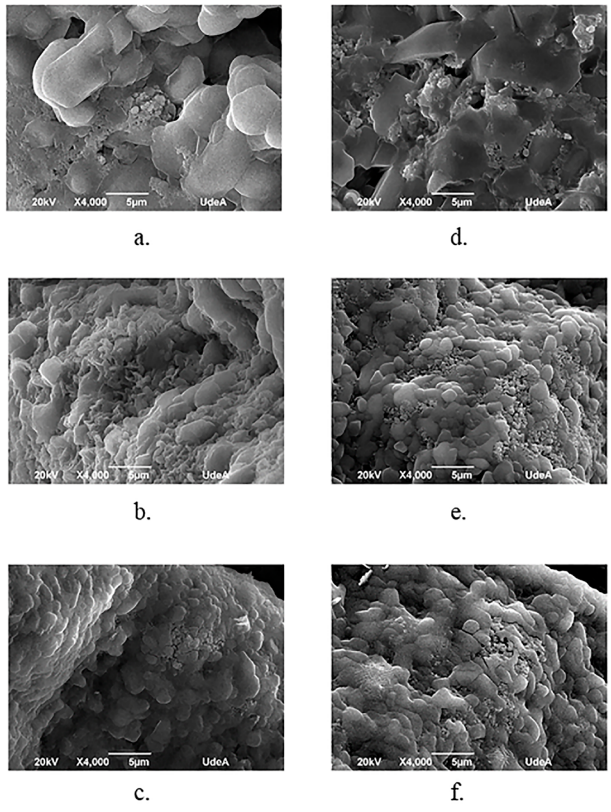

Figure 5. SEM images after DSC and MDSC evaluation. a, b, and c represent samples that were evaluated by DSC with 0,5, 1,0, and 1,5 wt.% of alumina nanoparticles, respectively; and d, e, and f are samples evaluated by MDSC with 0,5, 1,0, and 1,5 wt.% of alumina nanoparticles, respectively.
Source: Authors

other authors have reported an enhancement in specific heat capacity in the absence of a particular network, which may be due to the fact that Cp is a structure-insensitive property (Chieruzzi *et al.*, 2017a; Myers *et al.*, 2016). Thus, it can be stated that these structures are not the only factors affecting the increment of the specific heat capacity,

and it is therefore necessary to evaluate other factors that may explain the specific heat increase. By comparing the SEM images of the base HITEC (Figure 4) with the MSBNFs evaluated by DSC and MDSC (Figure 5), it is possible to observe a reduction in the grain size as the proportion of nanoparticles within it increases and the salt coalesces. It could be said that the nanoparticles are fulfilling the role of a nucleating agent. This could be linked to the increase in Cp of the MSBNFs. A similar behavior has been reported by other authors (Ho and Pan, 2014).

It is important to highlight that the microstructure of the MSBNFs is independent of the technique used to evaluate the specific heat capacity, be it DSC or MDSC. A similar morphology was also observed by other authors in a similar type of nanofluid (Chieruzzi *et al*., 2017a). Additionally, this method has the advantage of replacing the water with butanol, thus reducing the time of evaporation, and ensuring a good suspension of the nanoparticles in the alcohol before they mix with the molten salt. Possible explanations for this behavior could be the use of high-energy milling at 300 rpm for 15 minutes, which ensures good homogeneity of the molten salt and good suspension of the nanoparticles in the butanol before mixing with the molten salt; and thermal cycling, which ensures good homogeneity in the final mixture.

Conclusions

In this study, a two-step method which replaces water with butanol and uses an Emax high-energy mill to prepare molten salt-based nanofluids is proposed. HITEC molten salt was used as the base fluid with different mass fractions of Al_2O_3 nanoparticles. The thermal properties, namely melting point, specific heat capacity, and thermal stability, of the commercial molten salt and the MSBNFs were experimentally tested. The conclusions obtained are presented in this section.

According to the results, it was possible to demonstrate the viability of the synthesis of the molten salt-based nanofluids through the aforementioned method, as evidenced in the increase in specific heat capacity of up to 0,53% when measured by DSC and of 4,57% when evaluated by MDSC for 1,0 wt.% of alumina nanoparticles. The thermal stability was not affected and a melting point reduction was obtained for this sample. Similarly, a good distribution of the nanoparticles was evident in all mass fractions of alumina, especially in 1,0 wt.%, which showed a Cp higher than the other compositions evaluated. Hence, it may be stated that a better distribution of smaller aggregates tends to be correlated with an increase in specific heat capacity.

The specific heat capacity (Cp) values of both the HITEC commercial molten salt and the nanofluids were evaluated by two different methods: traditional differential scanning calorimetry (DSC) and modulated differential scanning calorimetry (MDSC). The enhancement percentage measured by the DSC method with all proportions of nanoparticles was not significant in comparison with the Cp of the pure HITEC salt. This behavior could indicate that there is no effect caused by the addition of this type of nanoparticle, which contradicts recent studies. On the other hand, the MDSC method showed a greater variation in the enhancement percentage, thus indicating that there is a positive effect attributable to the nanoparticles, in addition to a greater sensitivity of this technique to small changes in the sample, especially in non-homogeneous samples such as nanofluids. This establishes the contribution of the two phases that make up the nanofluid, the molten salt as the base fluid and the solid nanoparticles. For this reason, the MDSC technique could be more appropriate for measuring this property in this type of sample. Similarly, the heating rate used in each of the techniques can influence the sensitivity to determine changes in nanofluids.

The good distribution of the nanoparticles, together with an increase in specific heat capacity without affecting thermal stability and a reduction in the melting point, demonstrate that the proposed two-step method is viable for manufacturing molten salt-based nanofluids while avoiding the use of water and therefore its subsequent elimination, thus reducing costs and production times, without having a great influence on the dispersion and homogenization of the nanofluid. Hence, the storage capacity of the nanofluid is increased to improve the thermal storage systems of CSP plants.

Acknowledgments

The authors, particularly Marllory Isaza-Ruiz, are grateful for the financial support provided through Doctoral Grant number 727–2015 by means of the Ministry of Science, Technology, and Innovation [*Ministerio de Ciencia, Tecnología e Innovación, Minciencias*].

References

Andreu-Cabedo, P., Mondragón, R., Hernández, L., Martínez-Cuenca, R., Cabedo, L., and Julia, J. E. (2014). Increment of specific heat capacity of solar salt with SiO_2 nanoparticles. *Nanoscale Research Letters*, 9(1), 582. https://doi.org/10.1186/1556-276X-9-582

ASTM International (2011). *E1269: Standard test method for determining specific heat capacity by differential scanning*. ASTM International. https://doi.org/10.1520/E1269-11.2

ASTM International (2015). *E2716-09: Standard test method for determining specific heat capacity by sinusoidal modulated temperature differential scanning calorimetry*. ASTM International. https://doi.org/10.1520/E2716-09R14.2

Awad, A., Navarro, H., Ding, Y., and Wen, D. (2018). Thermal-physical properties of nanoparticle-seeded nitrate molten salts. *Renewable Energy*, *120*, 275-288. https://doi.org/10.1016/j.renene.2017.12.026

Betts, M. R. (2011). *The effects of nanoparticle augmentation of nitrate thermal storage materials for use in concentrating solar power applications* [Master's thesis, Texas A&M University]. https://hdl.handle.net/1969.1/ETD-TAMU-2011-05-9118

Bonk, A., Sau, S., Uranga, N., Hernaiz, M., and Bauer, T. (2018). Advanced heat transfer fluids for direct molten salt line-focusing CSP plants. *Progress in Energy and Combustion Science*, *67*, 69-87. https://doi.org/10.1016/j.pecs.2018.02.002

Botero, Y. L., López-Rendón, J. E., Ramírez, D., Zapata, D. M., and Jaramillo, F. (2020). From clay minerals to Al2O3 nanoparticles: Synthesis and colloidal stabilization for optoelectronic applications. *Minerals*, *10*(2), 118. https://doi.org/10.3390/min10020118

Chen, X., Wu, Y. ting, Zhang, L. di, Wang, X., and Ma, C. fang. (2018). Experimental study on the specific heat and stability of molten salt nanofluids prepared by high-temperature melting. *Solar Energy Materials and Solar Cells*, *176*, 42-48. https://doi.org/10.1016/j.solmat.2017.11.021

Chen, X., Wu, Y. ting, Zhang, L. di, Wang, X., and Ma, C. fang. (2019). Experimental study on thermophysical properties of molten salt nanofluids prepared by high-temperature melting. *Solar Energy Materials and Solar Cells*, *191*, 209-217. https://doi.org/10.1016/j.solmat.2018.11.003

Chieruzzi, M., Cerritelli, G. F., Miliozzi, A., and Kenny, J. M. (2013). Effect of nanoparticles on heat capacity of nanofluids based on molten salts as PCM for thermal energy storage. *Nanoscale Research Letters*, *8*(1), 448. https://doi.org/10.1186/1556-276X-8-448

Chieruzzi, M., Cerritelli, G. F., Miliozzi, A., Kenny, J. M., and Torre, L. (2017a). Heat capacity of nanofluids for solar energy storage produced by dispersing oxide nanoparticles in nitrate salt mixture directly at high temperature. *Solar Energy Materials and Solar Cells*, *167*, 60-69. https://doi.org/10.1016/j.solmat.2017.04.011

Chieruzzi, M., Cerritelli, G. F., Miliozzi, A., Kenny, J. M., and Torre, L. (2017b). Heat capacity of nanofluids for solar energy storage produced by dispersing oxide nanoparticles in nitrate salt mixture directly at high temperature. *Solar Energy Materials and Solar Cells*, *167*, 60-69. https://doi.org/10.1016/j.solmat.2017.04.011

Coastal Chemical Co. LLC. (2009). *HITEC ® Heat Transfer Salt*. http://www.skyscrubber.com/MSR%20-%20HITEC%20Heat%20Transfer%20Salt.pdf

Dudda, B., and Shin, D. (2013). Effect of nanoparticle dispersion on specific heat capacity of a binary nitrate salt eutectic for concentrated solar power applications. *International Journal of Thermal Sciences*, *69*, 37-42. https://doi.org/10.1016/j.ijthermalsci.2013.02.003

Fernández, A. G., Galleguillos, H., Fuentealba, E., and Pérez, F. J. (2015). Thermal characterization of HITEC molten salt for energy storage in solar linear concentrated technology. *Journal of Thermal Analysis and Calorimetry*, *122*(1), 3-9. https://doi.org/10.1007/s10973-015-4715-9

Gimenez, P., and Fereres, S. (2015). Effect of heating rates and composition on the thermal decomposition of nitrate based molten salts. *Energy Procedia*, *69*, 654-662. https://doi.org/10.1016/j.egypro.2015.03.075

Ho, M. X., and Pan, C. (2014). Optimal concentration of alumina nanoparticles in molten hitec salt to maximize its specific heat capacity. *International Journal of Heat and Mass Transfer*, *70*, 174-184. https://doi.org/10.1016/j.ijheatmasstransfer.2013.10.078

Ho, M. X., and Pan, C. (2017). Experimental investigation of heat transfer performance of molten HITEC salt flow with alumina nanoparticles. *International Journal of Heat and Mass Transfer*, *107*, 1094-1103. https://doi.org/10.1016/j.ijheatmasstransfer.2016.11.015

Hu, Y., He, Y., Zhang, Z., and Wen, D. (2017). Effect of Al2O3 nanoparticle dispersion on the specific heat capacity of a eutectic binary nitrate salt for solar power applications. *Energy Conversion and Management*, *142*, 366-373. https://doi.org/10.1016/j.enconman.2017.03.062

Hu, Y., He, Y., Zhang, Z., and Wen, D. (2019). Enhanced heat capacity of binary nitrate eutectic salt-silica nanofluid for solar energy storage. *Solar Energy Materials and Solar Cells*, *192*, 94-102. https://doi.org/10.1016/j.solmat.2018.12.019

Kearney, D., Herrmann, U., Nava, P., Kelly, B., Mahoney, R., Pacheco, J., Cable, R., Potrovitza, N., Blake, D., and Price, H. (2002). Assessment of a molten salt heat transfer fluid in a parabolic trough solar field. *Journal of Solar Energy Engineering*, *125*(2), 170-176. https://doi.org/10.1115/1.1565087

Larche, F. C. (1945). Melting point of alpha-alumina. *Journal of the Franklin Institute*, *139*(5), 406. https://www.sciencedirect.com/science/article/abs/pii/0016003245900238

Lu, M.-C., and Huang, C.-H. (2013). Specific heat capacity of molten salt-based alumina nanofluid. *Nanoscale Research Letters*, *8*(1), 292. https://doi.org/10.1186/1556-276X-8-292

Mohammad, M. Bin, Brooks, G. A., and Rhamdhani, M. A. (2017). Thermal analysis of molten ternary lithium-sodium-potassium nitrates. *Renewable Energy*, *104*, 76-87. https://doi.org/10.1016/j.renene.2016.12.015

Muñoz-Sánchez, B., Nieto-Maestre, J., Guerreiro, L., Julia, J. E., Collares-Pereira, M., and García-Romero, A. (2017). Molten salt based nanofluids based on solar salt and alumina nanoparticles: An industrial approach. *AIP Conference Proceedings*, *1850,* 080016. https://doi.org/10.1063/1.4984437

Muñoz-Sánchez, B., Nieto-Maestre, J., Imbuluzqueta, G., Marañón, I., Iparraguirre-Torres, I., and García-Romero, A. (2017). A precise method to measure the specific heat of solar salt-based nanofluids. *Journal of Thermal Analysis and Calorimetry*, *129*(2), 905-914. https://doi.org/10.1007/s10973-017-6272-x

Muñoz-Sánchez, B., Nieto-Maestre, J., Veca, E., Liberatore, R., Sau, S., Navarro, H., Ding, Y., Navarrete, N., Juliá, J. E., Fernández, A. G., and García-Romero, A. (2018). Rheology of Solar-Salt based nanofluids for concentrated solar power. Influence of the salt purity, nanoparticle concentration, temperature and rheometer geometry. *Solar Energy Materials and Solar Cells*, *176*, 357-373. https://doi.org/10.1016/j.solmat.2017.10.022

Myers, P. D., Alam, T. E., Kamal, R., Goswami, D. Y., and Stefanakos, E. (2016). Nitrate salts doped with CuO nanoparticles for thermal energy storage with improved heat transfer. *Applied Energy*, *165*, 225-233. https://doi.org/10.1016/j.apenergy.2015.11.045

Navarrete, N., Hernández, L., Vela, A., and Mondragón, R. (2020). Influence of the production method on the thermophysical properties of high temperature molten salt-based nanofluids. *Journal of Molecular Liquids*, *302,* 112570. https://doi.org/10.1016/j.molliq.2020.112570

REN21 (2021). *Renewables 2021 Global Status Report*. https://abdn.pure.elsevier.com/en/en/researchoutput/ren21(-5d1212f6-d863-45f7-8979-5f68a61e380e).html

Schuller, M., Shao, Q., and Lalk, T. (2015). Experimental investigation of the specific heat of a nitrate-alumina nanofluid for solar thermal energy storage systems. *International Journal of Thermal Sciences*, *91*, 142-145. https://doi.org/10.1016/j.ijthermalsci.2015.01.012

Seo, J., and Shin, D. (2016). Size effect of nanoparticle on specific heat in a ternary nitrate ($LiNO_3$-$NaNO_3$-KNO_3) salt eutectic for thermal energy storage. *Applied Thermal Engineering*, *102*, 144-148. https://doi.org/10.1016/j.applthermaleng.2016.03.134

Serrano-López, R., Fradera, J., and Cuesta-López, S. (2013). Molten salts database for energy applications. *Chemical Engineering and Processing*, *73*, 87–102. https://doi.org/10.1016/j.cep.2013.07.008

Shin, D., and Banerjee, D. (2014). Specific heat of nanofluids synthesized by dispersing alumina nanoparticles in alkali salt eutectic. *International Journal of Heat and Mass Transfer*, *74*, 210-214. https://doi.org/10.1016/j.ijheatmasstransfer.2014.02.066

Song, W., Lu, Y., Wu, Y., and Ma, C. (2018). Effect of SiO_2 nanoparticles on specific heat capacity of low-melting-point eutectic quaternary nitrate salt. *Solar Energy Materials and Solar Cells*, *179*, 66-71. https://doi.org/10.1016/j.solmat.2018.01.014

Tiznobaik, H., and Shin, D. (2013). Enhanced specific heat capacity of high-temperature molten salt-based nanofluids. *International Journal of Heat and Mass Transfer*, *57*(2), 542548. https://doi.org/10.1016/j.ijheatmasstransfer.2012.10.062

Vignarooban, K., Xu, X., Arvay, A., Hsu, K., and Kannan, A. M. (2015). Heat transfer fluids for concentrating solar power systems - A review. *Applied Energy*, *146*, 383-396. https://doi.org/10.1016/j.apenergy.2015.01.125

Villada, C., Bonk, A., Bauer, T., and Bolívar, F. (2018). High-temperature stability of nitrate/nitrite molten salt mixtures under different atmospheres. *Applied Energy, 226,* 107-115. https://doi.org/10.1016/j.apenergy.2018.05.101

Villada, C., Jaramillo, F., Castaño, J. G., Echeverría, F., and Bolívar, F. (2019). Design and development of nitrate-nitrite based molten salts for concentrating solar power applications. *Solar Energy*, *188*, 291-299. https://doi.org/10.1016/j.solener.2019.06.010

Zhang, S., Wu, W., and Wang, S. (2017). Integration highly concentrated photovoltaic module exhaust heat recovery system with adsorption air-conditioning module via phase change materials. *Energy*, *118*, 1187-1197. https://doi.org/10.1016/j.energy.2016.10.139